LVIS553 Transcriptional Regulator Specifically Recognizes Novobiocin as an Effector Molecule*[S]

Fernando A. Pagliai, Christopher L. Gardner, Santosh G. Pande, and Graciela L. Lorca[1]

From the Department of Microbiology and Cell Science, Genetics Institute, Institute of Food and Agricultural Sciences, University of Florida, Gainesville, Florida 32610-3610

In this study we aimed to identify small molecules with high affinity involved in the allosteric regulation of LVIS553, a MarR member from *Lactobacillus brevis* ATCC367. Using high throughput screening, novobiocin was found to specifically bind LVIS553 with a $K_D = 33.8 \pm 2.9$ μM consistent with a biologically relevant ligand. Structure guided site-directed mutagenesis identified Lys[9] as a key residue in novobiocin recognition. The results found *in vitro* were correlated *in vivo*. An increased tolerance to the antibiotic was observed when LVIS553 and the downstream putative transport protein LVIS552 were either expressed in a low copy plasmid in *L. brevis* or as a single copy chromosomal insertion in *Bacillus subtilis.* We provide evidence that LVIS553 is involved in the specific regulation of a new mechanism of tolerance to novobiocin.

The MarR family of transcriptional regulators is a diverse group of small proteins (120–207 amino acids long) that share similar structural scaffold (1). Conversely, analysis of the amino acid sequence alignment of well characterized MarR members, such as MarR (PDB code 1JGS), OhrR (PDB code 1Z91), SlyA (PDB code 1LJ9), and EmrR (PDB code 2GXG) revealed that very few amino acids are conserved (2). Consequently, the main focus of several previous reports has been to further understand the contribution of conserved structures to DNA binding and the key roles of individual amino acids. As a result, the location of the MarR DNA binding domain was previously determined to reside within amino acids 61–121 (3). Further reports have shown that mutations on residues allocated in this area have both structural and functional consequences that decrease DNA binding as shown for MarR (3), SlyA in *Salmonella* (4), and MdtR (YusO) in *Bacillus subtilis* (5). To date, however, we are far from understanding in depth the molecular mechanisms behind the structural modifications associated with ligand binding.

Several factors have contributed to the uncertainties that remain regarding ligand binding. First and foremost, the ability to identify specific amino acids and their associated functional involvement has been hindered by the overlapping nature of both the DNA and ligand binding motifs. In addition, attempts to examine the mechanisms in detail have

been further hampered due to the overall lack of physiologically relevant ligands. Annotations for the majority of family members are usually based on *in silico* data without direct physiological evidence. The founding member of this family is MarR from *Escherichia coli* (6, 7), which has been biochemically, structurally, and phenotypically characterized. MarR binds salicylate and other phenolic compounds such as plumbagin, 2,4-dinitrophenol, and menadione in the low millimolar range (0.5–2 mM) (8, 9).

Many orthologs have been reported thereafter and binding to salicylate has been claimed (10), although in most cases, their binding affinities are too low to be considered biologically or biochemically relevant. Other well characterized members of this family such as EmrR (11) and HucR bind small molecules in the low micromolar range (2.0–15.0 and 11.6 μM, respectively) (12, 13). Accordingly, we are particularly interested in identifying alternative ligands, elucidating the mechanisms by which small molecules regulate the formation and release of transcriptional regulators from the cognate DNA sequence, and discussing the molecular results under the light of its physiological consequences.

Due to their involvement in multidrug resistance and tolerance to highly toxic compounds, MarR members have been predominately studied in pathogenic microorganisms, although they are found throughout many bacterial and archaeal groups (14). It is particularly interesting to determine how commensal bacteria such as *Lactobacillus* are able to tolerate and survive antibiotics as a means of persistence in the intestinal tract or as a competitive advantage over other commensal members. Lactobacilli are in general, very resistant and capable of tolerating a wide variety of stress conditions (for a review, see Lorca and Font de Valdez (15)). *Lactobacillus brevis*, in particular, has received a lot of attention due to its role in spoilage of beer (16), which involves induction of efflux pumps as a mechanism of hop resistance (17, 18). By comparative genomics we determined that *L. brevis* has the highest number of transport proteins (13%) involved in the uptake and efflux of drugs and toxic compounds (19, 20). Collectively, these characteristics make *L. brevis* a good model for understanding how commensal bacteria respond to environmental stressors such as antibiotics, via mechanisms in which transcriptional regulators may be involved.

In this study we used LVIS553 as a model protein to locate and examine high affinity small molecules involved in the allosteric regulation of a MarR member. The identified molecule, novobiocin, was found to specifically bind LVIS553 in the low

micromolar range. We provide *in vivo* evidence that LVIS553 is involved in the regulation of a new mechanism of tolerance to novobiocin.

EXPERIMENTAL PROCEDURES

Bacterial Strains—*L. brevis* ATCC367 was obtained from the American Type Culture Collection (Manassas, VA). *Lactobacillus* strains were grown at 37 °C in MRS broth (Difco Laboratories, Detroit, MI). *E. coli* DH5α cells, used to carry and propagate all vectors, were grown in Luria-Bertani medium (Difco). *B. subtilis* M168 was used for heterologous gene expression. Growth was performed in LB medium at 37 °C under aerobic conditions. When appropriate, medium was supplemented with erythromycin (7.5 μg/ml) (for *L. brevis*), kanamycin (5 μg/ml) (for *B. subtilis*), or ampicillin (100 μg/ml) (for *E. coli*). All antibiotics and chemicals were purchased from Sigma.

DNA Manipulations and Gene Cloning—Standard methods were used for site-directed mutagenesis, chromosomal DNA isolation, restriction enzyme digestion, agarose gel electrophoresis, ligation, and transformation (21). Plasmids were isolated using spin miniprep kits (Qiagen, Valencia, CA) and PCR products were purified using QIAquick purification kits (Qiagen). Mutagenesis was performed using the QuikChange Site-directed Mutagenesis kit (Stratagene, La Jolla, CA).

For protein expression and purification, the *LVIS553* gene was amplified from *L. brevis* ATCC367 chromosomal DNA by PCR. The primers utilized are described in Table 1. The plasmid p15TV-L (GenBank accession EF456736) obtained from the Structural Genomics Consortium (SGC, Toronto) was employed as a vector. This construct also provides a N-terminal hexahistidine tag, separated from the protein by a tobacco etch virus protease recognition site (ENLYFQ ↓ GS).

Cloning in the pRV610 plasmid (22) was performed amplifying *LVIS552-LVIS553* (including the complete $P_{LVIS553}$) by PCR, using the primers described in Table 1. Clones were confirmed by sequencing using universal M13 primers.

For heterologous gene expression of *L. brevis* genes in *B. subtilis*, *LVIS552-LVIS553* was amplified using PCR, cut with KpnI and XbaI restriction enzymes, and cloned in pSac-Kan (23). Recombinant clones were obtained in *E. coli* DH5α and subsequently sequenced. Transformation of *B. subtilis* was performed by natural competence. Integration in the *sacA* gene was verified by the inability to utilize sucrose as a carbon source on minimal medium (24).

Protein Purification—Protein purification was carried out as previously described (25). Briefly, the His-tagged fusion proteins were overexpressed in *E. coli* BL21-Star(DE3) cells (Stratagene). The cells were grown in LB at 37 °C to an A_{600} ~0.6 and expression induced with 0.4 mM isopropyl 1-thio-β-D-galactopyranoside. After addition of isopropyl 1-thio-β-D-galactopyranoside, the cells were incubated with shaking at 15 °C overnight. The cells were harvested, resuspended in binding buffer (500 mM NaCl, 5% glycerol, 50 mM HEPES, pH 7.5, 5 mM imidazole), flash frozen in liquid N_2, and stored at −70 °C. The thawed cells were lysed and passed through a French Press after the addition of 0.5% Nonidet P-40 and 1 mM each of phenylmethylsulfonyl fluoride and benzamidine. The lysate was clarified by centrifugation (30 min at 17,000 × *g*) and applied to a metal chelate affinity column charged with Ni^{2+}. After the column was washed and the protein was eluted from the column in elution buffer (binding buffer with 500 mM imidazole). The His_6 tag was then cleaved from the protein by treatment with recombinant His-tagged tobacco etch virus protease. The cleaved protein was resolved from the cleaved His tag and the His-tagged protease by passing the mixture through a second Ni^{2+} column. The purified proteins were dialyzed against 10 mM HEPES, pH 7.5, 500 mM NaCl, and concentrated using a BioMax concentrator (Millipore, Billerica, MA).

Size Exclusion Chromatography—A 100-μl protein sample contained 10 mM HEPES, pH 7.5, 500 mM NaCl, 25 μM LVIS553, and where indicated, 100 μM novobiocin. Following a 20-min incubation on ice, samples were injected onto a Superose 12 10/300 GL gel filtration column (Amersham Biosciences) installed on an Äkta system (Amersham Biosciences) equilibrated with 10 mM HEPES, pH 7.5, 500 mM NaCl. Filtration was performed at 4 °C at a flow rate of 0.5 ml/min and the protein concentration was monitored by measuring the absorbance at 280 nm. Blue dextran 2000 was used to determine the void volume. A mixture of protein molecular mass standards, containing β-amylase (200 kDa), bovine serum albumin (66 kDa), carbonic anhydrase (29 kDa), and cytochrome *c* (12.4 kDa), was applied to the column under similar conditions. The elution volumes and molecular masses of the protein standards

TABLE 1
Oligonucleotides used in this work

Primer	To LVIS553 ATG	Oligonucleotide sequence (5′ → 3′)
Protein purification		
LB45 Fw	...+1...	*ttgtatttccagggc*atgactcaacccattacctttaata aatatattg[a]
LB45 Rv	...+438...	*caagcttcgtcatca*tcagttcctttcttgtcgctgttg[a]
EMSA		
PLvis552 Fw[b]	...+724...	aaaactcatggcgcagaaag
PLvis552 Rv	...+489...	aacaacttgcggccatttac
PLvis553 Fw[b]	...+24...	attaaaggtaatgggttgagtcat
PLvis553 Rv	...−273...	gtgcggacctcctttgaat
PLvis553-Int Fw[b]	...+203...	aagtcacgagcgaccagact
PLvis553-Int Rv	...−134...	gaagacccatttgcgttgaa
PLvis554 Fw[b]	...−107...	atcgtttttcaacgcaaatgg
PLvis554 Rv	...−411...	gccttaacaccaagggtttg
Site-directed mutagenesis		
Lvis553_K9A Fw	...+7...	caacccattacctttaatgcatatattgccagtatttac
Lvis553_K9A Rv	...+45...	gtaaatactggcaatatatgcattaaaggtaatgggttg
Lvis553_R16A Fw	...+28...	tatattgccagtatttacgcccaatctaagcatgacttc
Lvis553_R16A Rv	...+66...	gaagtcatgcttagattgggcgtaaatactggcaatata
Cloning into pRV610		
Lvis552–553 KpnI Fw	...+1152...	ggggtaccgaatcagtctggctgggaag[c]
Lvis552–553 XbaI Rv	...−272...	gctctagagcggacctcctttgaatttt[c]
Competition assay		
Lvis553 protection Fw	...−18...	aaaaaatagtggataagtccattaaattct
Lvis553 protection Rv	...−47...	agaatttaatggacttatccactattttt
DNase I footprinting		
Lvis553fprint_*FAM* Rv	...+203...	aagtcacgagcgaccagact
Lvis553fprint_*VIC* Fw	...−273...	gtgcggacctcctttgaat
Quantitative reverse transcription-PCR		
Lvis552 Fw	...+550...	tcgccaatttctagcattcc
Lvis552 Rv	...+718...	caccgaaaataacggaagga
Lvis553 Fw	...+4...	actcaacccattacctttaat
Lvis553 Rv	...+435...	gttcctttcttgtcgctgttg
rpoD Fw		attcccgttcatatggtgga
rpoD Rv		gaacctttccgttgccata

[a] Italics show the extra bases added to the 5′ end for the ligation independent cloning using the BD-infusion CF Dry-Down PCR cloning kit (BD Biosciences).
[b] Biotin labeled.
[c] Underlines indicate the restriction sites.

were used to generate a standard curve from which the apparent molecular mass was determined.

Electrophoretic Mobility Shift Assays (EMSA)[2]—EMSA for LVIS553 was performed using protein purified and concentrated according to the procedures described above. Fragments for the $P_{LVIS552}$, $P_{LVIS553}$, and $P_{LVIS554}$ promoter regions (Table 1) were generated by PCR using biotin-prelabeled (5'-end) primers, then purified using QIAquick spin columns (Qiagen). Incubation mixtures for EMSA (20 μl) contained 2.5 nM of a 5'-labeled DNA fragment, 50 mM Tris-HCl, pH 7.5, 150 mM KCl, 10 mM MgCl, 0.01% Triton X-100, 50 ng/μl of poly(dI-dC) nonspecific competitor DNA, purified LVIS553 protein (0–100 nM), and ligand (0–1 mM) when indicated.

After incubation for 20 min at 37 °C, samples were separated on 6% acrylamide-bisacrylamide nondenaturing gels in 0.5× Tris borate-EDTA buffer, pH 8.3 (TBE). Electrophoresis was performed at 100 V using ice-cold 0.5× TBE as a running buffer. DNA was then transferred from the polyacrylamide gel to the Biodyne B Positive Nylon Membrane (Pierce) by electro-blotting at 380 mA for 40 min in 0.5× TBE. Transferred DNA was cross-linked for 15 min using a UV cross-linker equipped with 312-nm bulbs. Biotin-labeled DNA was detected using a horseradish peroxidase/Super Signal Detection System (Pierce). Membranes were exposed to Kodak x-ray film.

For EMSA competition assays, oligonucleotides corresponding to both strands of protected regions in the footprint assay (Table 1) were synthesized. Annealing was carried out by mixing equimolar amounts (at a concentration of 100 μM) of each complementary oligonucleotide in 0.25 M Tris-HCl, pH 8.0. The mixture was incubated at 95 °C for 5 min and then chilled on ice.

DNase I Footprinting—DNase I footprint assay was carried out as described previously by Zianni *et al.* (26) in the Plant and Microbe Genomics Facility at Ohio State University, Columbus, OH. Briefly, 5'-VIC or 5'-FAM-labeled probes were generated by PCR using the primers listed in Table 1. The reaction mixture containing 750 ng of labeled probe, 14 μg of LVIS553, 50 mM Tris-HCl, pH 7.5, 150 mM KCl, 12.5 mM MgCl$_2$, 0.5 mM CaCl$_2$, 0.01% Triton X-100, 25 ng/μl of poly(dI-dC)-nonspecific competitor DNA, and 0.006 units of DNase I (New England Biolabs, Ipswich, MA) was incubated for 20 min at 37 °C. The reaction was terminated with 10 mM EDTA, pH 8.0. The mixture was heat inactivated at 72 °C for 10 min. The DNA fragments were purified with phenol/chloroform/isoamyl alcohol (ratio 25:24:1) and precipitated with ethanol. A non-digested fragment was used for sequencing reactions with the Thermo Sequence dye primer manual cycle sequencing kit (U. S. Biochemical Corp.). The digested DNA and sequencing reaction products were analyzed with a 3730 DNA analyzer and the protected regions were identified with GeneMarker (Soft genetics).

Quantitative Reverse Transcription-PCR Studies—Bacterial cells were cultured in MRS broth with novobiocin (0.5 or 1 μM) or coumermycin A1 (0.1 or 0.5 μM) when required. The cells were collected by centrifugation at 4 °C when A_{600} ~0.5. Total

RNA was subsequently isolated with RiboPure™-Bacteria (Ambion, Austin, TX) in accordance with the manufacturer's protocol. cDNAs were synthesized with the Superscript™ first-strand synthesis kit (Invitrogen) in accordance with the manufacturer's instructions and stored at −80 °C prior to use. Real time quantitative PCR was carried out on the iCycler IQ™ apparatus (Bio-Rad) using Platinum® SYBR® Green qPCR SuperMix for iCycler (Invitrogen) in accordance with the manufacturer's recommended protocol. Quantitative reverse transcription-PCR primers *LVIS552* and *LVIS553* are described in detail in Table 1. The *rpoD* gene was used as an internal control.

Small Molecule Screening by Differential Scanning Fluorimetry—Purified LVIS553 protein was screened against a library of 160 intracellular compounds (27) at a final concentration of 100 μM or against the Prestwick chemical library of 1152 compounds (Prestwick Chemical, France) at a final concentration of 1.3 μg/ml using fluorometry as previously described (27, 28). LVIS553 was diluted to a final concentration of 10 μM in 100 mM HEPES, pH 7.5, 150 mM NaCl. 25-μl aliquots of a protein solution containing the chemical compounds were placed in duplicate into 96-well plates (Bio-Rad) and heated from 25 to 80 °C at the rate of 1 °C per minute. A real time PCR device (iCycler IQ™, Bio-Rad) was used to monitor protein unfolding by an increase in the fluorescence of the fluorophor SYPRO Orange (Invitrogen). Fluorescence intensities were plotted against temperature for each sample well and transition curves were fitted using the Boltzmann equation using Origin 8 software (Northampton, MA). The midpoint of each transition was calculated and compared with the midpoint calculated for the reference sample. If the difference between them was greater than 2.0 °C, the corresponding compound was considered to be a "hit" and the experiment was repeated to confirm the effect in a dose-dependent manner.

Isothermal Titration Calorimetry—Measurements were performed on a VP-Microcalorimeter (MicroCal, Northampton, MA) at 30 °C. The protein was thoroughly dialyzed against 10 mM HEPES, pH 7.5, and 500 mM NaCl. A solution of novobiocin (1 mM) was directly prepared in dialysis buffer. Each titration involved a series of 4-μl injections of effector molecule into the protein solution. The mean enthalpies measured from injection of the ligand in the buffer were subtracted from raw titration data prior to data analysis with ORIGIN software (MicroCal). Titration curves were fitted by a nonlinear least squares method to a function for the binding of a ligand to a macromolecule (29). From the curve thus fitted, the parameters ΔH (reaction enthalpy), K_A (binding constant, $K_A = 1/K_D$), and n (reaction stoichiometry) were determined. From the values of K_A and ΔH, the changes in free energy (ΔG) and entropy (ΔS) were calculated with the equation: $\Delta G = -RT \ln K_A = \Delta H - T\Delta S$, where R is the universal molar gas constant and T is the absolute temperature.

RESULTS

LVIS553 Operon Structure and Binding Site—In *L. brevis* the MarR family (COG1846) is the most abundant and the most diverse group with 22 proteins or 15.4% of all transcription factors. These data correlate well with the high amount of drug efflux systems (13% of the total transport proteins)

---

[2] The abbreviations used are: EMSA, electrophoretic mobility shift assay; SAL1, salicylate binding pocket 1.
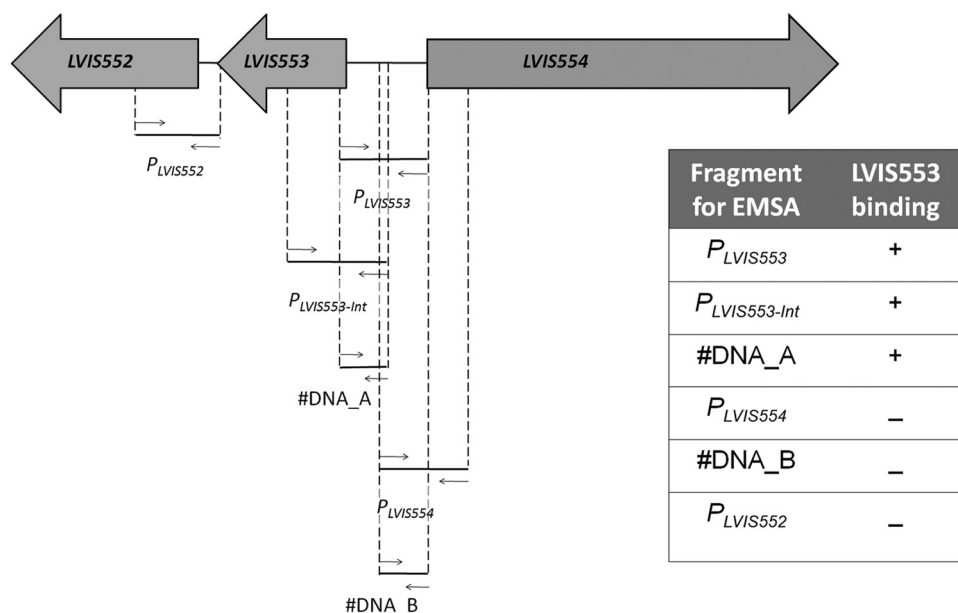
FIGURE 1. **Identification of the *LVIS553* binding site.** The genomic environment of *LVIS553* was extracted and analyzed to identify putative binding regions. Two membrane proteins were encoded upstream and downstream of *LVIS553*. Different primer combinations (Table 1) were used to determine the smallest DNA binding region for LVIS553. EMSA results are summarized in the *inset*. +, positive binding of LVIS553 using 10 nM pure protein; −, negative binding using up to 500 nM purified LVIS553 protein.

Fragment for EMSA	LVIS553 binding
$P_{LVIS553}$	+
$P_{LVIS553-Int}$	+
#DNA_A	+
$P_{LVIS554}$	−
#DNA_B	−
$P_{LVIS552}$	−

found in the genomes of *Lactobacillus* (19, 20). In this report, we chose LVIS553 as our model protein for the first step in unveiling small regulatory molecules for this diverse group of proteins.

To determine the binding site for LVIS553, the genomic environment was analyzed (Fig. 1). *LVIS553* is encoded in the minus strand and *LVIS554* is encoded downstream on the plus strand. This protein is annotated as a putative Na$^+$-driven multidrug efflux pump and classified using the Transport Classification Data base (30) within the multi-antimicrobial extrusion (MATE) family, TCDB 2.A.66.1. Upstream of *LVIS553* on the minus strand is *LVIS552*, which encodes for a protein with four predicted transmembrane domains. No characterized homologs of *LVIS552* were identified on either TCDB or nonredundant databases. The genomic environment of *LVIS552-LVIS553*, however, was found to be conserved in *Lactobacillus plantarum,* but not in other *Lactobacillus*. Interestingly, the only two other genomes where this putative operon is conserved is in *Ruminococcus obeum* and *Blautia hydrogenotrophica*. *LVIS554* shares a 64% identity at the protein level with the gene *lp_1386*, which is located in a different genomic environment than *lp_0816* and *lp_0817* (homologs to *LVIS552* and *LVIS553*, respectively), suggesting that they do not belong to the same transcriptional unit.

Based on the vast literature available in which local transcriptional regulators are usually encoded upstream or downstream of the regulated genes, we amplified by PCR two fragments: the first includes the intergenic region between *LVIS552* and *LVIS553* ($P_{LVIS552}$) and the second harbors the *LVIS553-LVIS554* ($P_{LVIS553}$) (Fig. 1). The protein-DNA interaction was tested by EMSA. We found that LVIS553 binds to $P_{LVIS553}$ but not to $P_{LVIS552}$ (Fig. 1). To narrow down the binding site we tested different combinations of primers within $P_{LVIS553}$

including the promoter-like region upstream of *LVIS554*. The smallest region that binds LVIS553 was found within 130 bp of the predicted start codon of *LVIS553*.

To determine the binding site of LVIS553, a DNase I footprinting assay was performed. We detected a protected region of 30 nucleotides located from base +13 to base −17 of both the plus and minus strands according to the +1 position of the predicted transcription start site (Fig. 2*A*). LVIS553 appears to protect a region that contains the predicted −10 region of $P_{LVIS553}$ as well as the hypothetical transcription start site (Fig. 2*B*). This protected region includes one imperfect inverted repeat (5′-TAaTGGAct-taTCCAcTA-3′) flanked on both sides by AT-rich sequences. The protected sequence also has two short mirror sequences, 5′-TTA-TCcaCTATT-3′ and 5′-AATTT-AAgAATTTAA-3′, that partially overlap the inverted repeats.

To confirm whether this protected region is the binding site for LVIS553, a competition assay was performed with the small, unlabeled double-stranded DNA of 30 bp, identified by DNase I footprinting. The LVIS553-$P_{LVIS553}$ interaction was incubated with increasing concentrations of this unlabeled DNA (FP-553). A 50% disruption of the LVIS553·$P_{LVIS553}$ complex was found at 1:1 ratio ($P_{LVIS553}$ DNA:FP-553 DNA) with a complete disruption at 1:10 ratio (Fig. 2*C*).

Screening of the Small Molecule Library for Binding to LVIS553—The expression of LVIS553 from *L. brevis* ATCC367 produced a soluble polypeptide (see "Experimental Procedures" for details) with an apparent molecular mass of 17.2 kDa and a yield of 12 mg/liters. LVIS553 was tested for binding against 158 metabolic scaffolds (31) and the Prestwick library by high-throughput protein stability assay, using fluorometry (27, 32). First, the thermal melt conditions for LVIS553 were established, to generate interpretable unfolding data (described under "Experimental procedures"). The midpoint transition was established at 56.6 °C. The compounds that induced a shift in the midpoint transition temperature (ΔT_m) of LVIS553 by more than 2.0 °C were considered hits. We found that LVIS553 showed an increase in T_m with carbamazepide ($\Delta T_m = 4.1$ °C), novobiocin ($\Delta T_m = 3.0$ °C), canrenoic acid ($\Delta T_m = 2.9$ °C), diazoxide ($\Delta T_m = 2.7$ °C), pindolol ($\Delta T_m = 2.5$ °C), and zomepirac ($\Delta T_m = 2.1$ °C) (Table 2). These results were confirmed by analyzing the dose dependence. This was accomplished by using increasing concentrations (0–1 mM) of each chemical. Interestingly, a common chemical scaffold was not identified among all hit molecules.

Effect of Putative Hits on DNA Binding in Vitro—The $P_{LVIS553}$ fragment was used to assess the effect of ligands on the protein-DNA interaction. Carbamazepine, canrenoic acid, diazox-
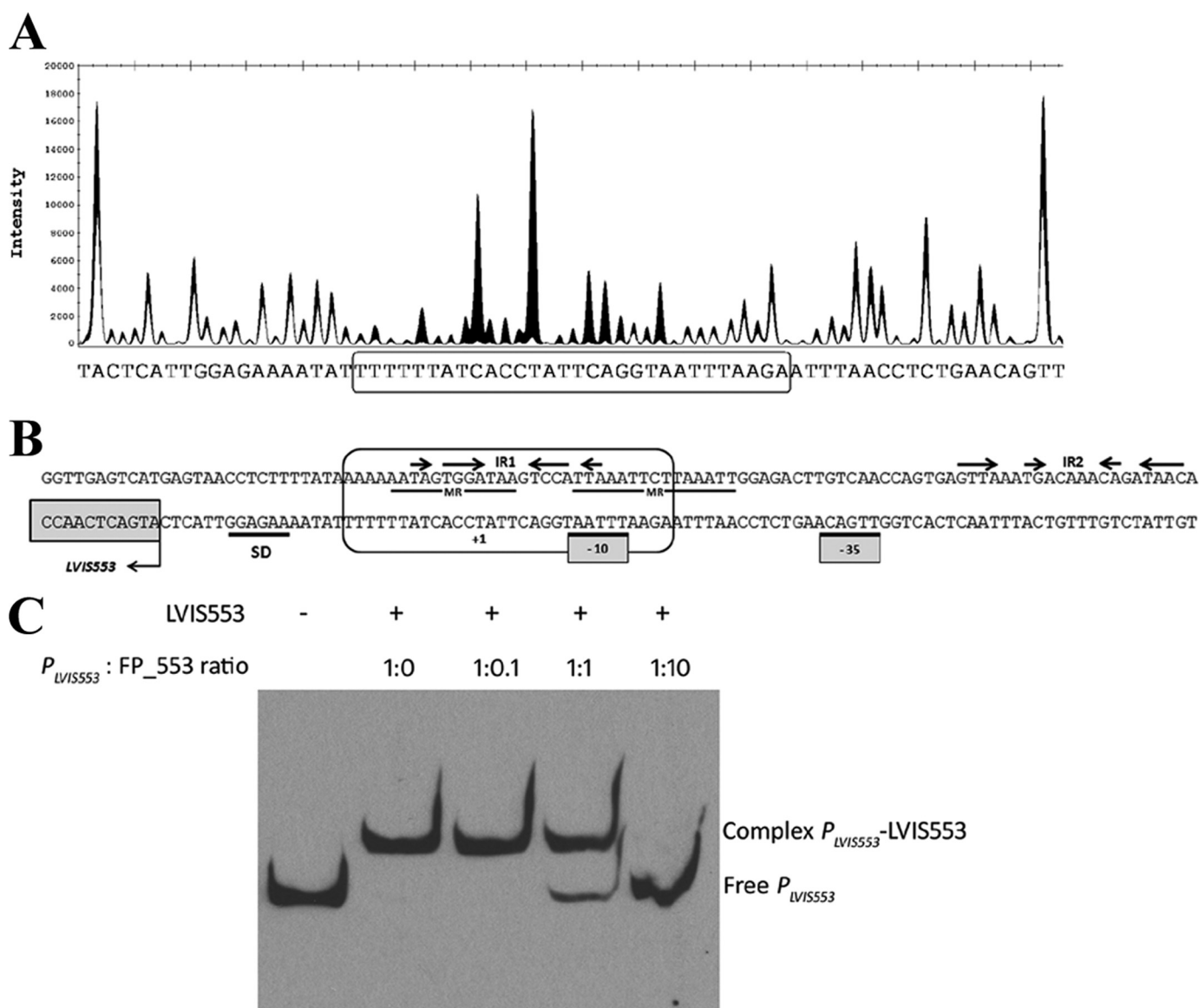
A

TACTCATTGGAGAAAATAT[TTTTTTTATCACCTATTCAGGTAATTTAAGA]ATTTAACCTCTGAACAGTT

B

C

FIGURE 2. **Analysis of the interaction between LVIS553 with the $P_{LVIS553}$ promoter.** *A*, DNase I footprinting. The electropherogram shows a fragment of the digested probe in the absence (*black*) or presence (*white*) of LVIS553 highlighting the protected region. The reaction mixture was treated as described under "Experimental Procedures" using as probe the primers shown under Table 1. The nucleotide sequence protected by LVIS553 is shown in the *bottom* of *panel A* and *boxed* in *B*. *B*, analysis of $P_{LVIS553}$ promoter. Predicted Shine-Dalgarno sequence and -10 and -35 of the $P_{LVIS553}$ are *underlined*. The protected regions of both plus and minus strands are indicated in a *circled box*. *IR*, inverted repeats; *MR*, mirror region. *C*, competition EMSA. Labeled $P_{LVIS553}$ promoter with 10 nM LVIS553 were mixed with increasing concentrations of unlabeled double-stranded FP-553 (30 bp-sequence identified by DNase I footprinting).

ide, zomepirac, and pindolol at 100 μM or 1 mM (Fig. 3*A*) had no effect on the binding ability of LVIS553 with $P_{LVIS553}$. According to EMSA results, novobiocin was the only ligand identified from screening that caused dissociation of LVIS553 from $P_{LVIS553}$ (Fig. 3*A*) in a concentration-dependent manner (Fig. 3*B*).

Using the structure of novobiocin as a model (33), we attempted to determine the smallest chemical scaffold that elicited an effect on LVIS553 using EMSA. We found that none of the coumarin-related molecules tested (coumarin, esculin, esculetin, umbelliferone, and scopoletin) had an effect on the stability of the LVIS553·$P_{LVIS553}$ complex when tested at 1 mM concentration (data not shown). Coumermycin A1 is a structurally related antibiotic that is also active on DNA gyrase (33). We determined the effect of coumermycin A1 on the binding of

LVIS553 to $P_{LVIS553}$ (Fig. 3*C*). EMSA experiments showed that coumermycin A1 is able to disrupt the DNA-protein complex at lower concentrations (50 μM) than novobiocin (100 μM).

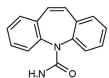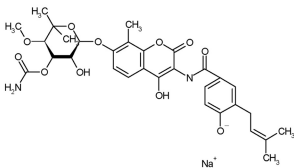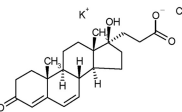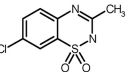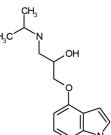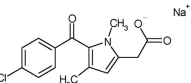*Modulation of LVIS553 Activity in Vivo*—The effect of novobiocin and coumermycin A1 on LVIS553 activity was assessed by measuring the expression of *LVIS553* and the downstream gene *LVIS552*. Cells were grown in MRS broth in the presence or absence of increasing concentrations of novobiocin (1 or 5 μM) or coumermycin A1 (0.1 or 0.5 μM). The difference in concentrations used for novobiocin and coumermycin A1 was due to higher sensitivity of *L. brevis* to the latter chemical. Novobiocin increased the expression of *LVIS553* ~2000-fold at 5 μM, whereas *LVIS552* was induced at a lower level (2-fold). Coumermycin A1 was found to be a weak inducer of *LVIS553* (24-fold) and had no effect on the expression of *LVIS552*

TABLE 2

Stabilization effect of ligand binding

The thermal stabilization of each protein by 0.1 μM ligand was evaluated using fluorometry.

Chemical	Delta temperature (°C)[1]	Chemical structure
Carbamazepine	4.1	
Novobiocin	3.0	
Canrenoic acid	2.9	
Diazoxide	2.7	
Pindolol	2.5	
Zomepirac	2.1	

[1] Delta temperature was calculated as the difference in the transition temperature between the protein in the absence and presence of a given ligand.

(supplemental Fig. S1). The difference in expression between LVIS552 and LVIS553 is intriguing because transcriptional terminators could not be identified in the intergenic region. These results indicate that although coumermycin A1 has an apparent higher affinity for LVIS553 *in vitro*, as shown on EMSA, the *in vivo* assays indicate that novobiocin might be the biologically relevant ligand for this transcriptional regulator.

To test this hypothesis, *LVIS552* and *LVIS553* genes (including the complete $P_{LVIS553}$) were cloned in the low copy vector pRV610 generating the pLVIS552_553 plasmid. The rationale being that if *L. brevis* ATCC 367 harbors a plasmid resulting in higher numbers of the transporter protein that mediate antibiotic efflux, an increased tolerance to novobiocin will be observed. *L. brevis*-pRV610 (*L. brevis* with empty plasmid as control) cells were grown with increasing concentrations of novobiocin (0.1–5 μM). An initial growth inhibition, indicated by a 60% decrease in the optical density with respect to a culture without novobiocin, was observed at 0.5 μM (Fig. 4*A*). This residual tolerance was not inhibited by concentrations up to 5 μM. Interestingly, *L. brevis*-pLVIS552_553 showed an increased tolerance (80% of the initial density) with 5 μM novobiocin (Fig. 4*A*). These results suggest that the putative transport protein LVIS552 is involved in the efflux of novobiocin. The residual tolerance observed at 0.5 μM in *L. brevis*-pRV610 could be explained by the activation of multiple unspecific drug efflux systems known to be abundant in the *L. brevis* genome (20).

Characterization of Novobiocin-LVIS553 Binding—To further characterize the LVIS553 interactions with the newly identified effector molecule, the thermodynamic properties of LVIS553 interactions with novobiocin were determined using isothermal titration calorimetry. The titration of LVIS553 followed an exothermal heat change profile giving rise to a hyperbolic binding curve (Fig. 5). Data were fitted with Origin software using the "one set of sites model." The derived thermodynamic parameters from the calorimetric titration of LVIS553 with novobiocin are as follows: $K_D = 33.8 \pm 2.9$, $n = 2$, $K_A = 2.7 \times E4$ M^{-1}, $\Delta H = -3.4 \pm 0.3$ kcal/mol, $T\Delta S = 50.3$ kcal/mol, $\Delta G = -506.5$ kcal/mol. In agreement with the results obtained through EMSA, the LVIS553 dissociation constant (K_D) for novobiocin is in the low micromolar range (33.8 ± 2.9 μM). Stoichiometry of the reaction is 2, which is consistent with the available crystallographic data on MTH313 from *Methanothermobacter thermautotrophicus* ΔH (2).

Although LVIS553 shares low sequence identity (21.6%) with MTH313, *in silico* modeling at Swiss-Model (34, 35) in the automated mode retrieved PDB code 3BPX (MTH313 with salicylate) as the best hit (*E*-value = 8.4e-19) (supplemental Fig. S2*A*). In MTH313, two distinctive binding sites were determined for salicylate. In salicylate binding pocket 1 (SAL1) (2) Lys[B8] and Arg[B16] make distinct contacts (ionic interactions or hydrogen bonds) with the salicylate molecule. These 2 amino acids are found at the junction of the dimerization domain and the DNA binding pocket (2). Lys[B8] and Arg[B16] of MTH313 are conserved in LVIS553 (Lys[9] and Arg[16]) (Fig. 6 and supplemental Fig. S2*B*). Interestingly, the predicted model of LVIS553 revealed that the orientation of the Lys[9] side chain is twisted toward the center of the binding pocket (Fig. 6). Amino acids with hydrophobic characteristics were also found in the MTH313 SAL1 pocket, which are also conserved in LVIS553. Based on the location of these residues, it was proposed that the binding of a salicylate molecule to MTH313 induces a structural change in the DNA binding motif of each monomer, resulting in the twisting out of the DNA binding lobes, decreasing the binding to DNA (2). In accordance with this model LVIS553 behaves as a dimer in solution with an apparent molecular mass of 34 kDa as determined by fast protein liquid chromatography separation (data not shown). The addition of different concentrations of novobiocin (10, 100, or 1000 μM) to either the reaction mixture or running buffer did not affect the oligomeric state of LVIS553, suggesting that a similar mechanism to MTH313 might be involved in molecular regulation by novobiocin.

An unbiased BLAST search (36) identified a large number (43) of homologs to LVIS553, with partial sequence alignment in which Arg[16] was conserved but Lys[9] was not (supplemental Fig. S2*B*). Based on these results it was hypothesized that Arg[16] might be involved in DNA binding, whereas Lys[9] might be involved in signal recognition. This was tested by changing Lys[9] and Arg[16] to either a small amino acid (alanine) or an acidic amino acid (aspartic acid). All these proteins were expressed in soluble form and tested by EMSA experiments. Mutations in Arg[16] (either to alanine or aspartic acid) rendered this protein unable to bind DNA, confirming that this amino acid is essential to DNA binding (Fig. 7*A*). Similarly, the mutant containing
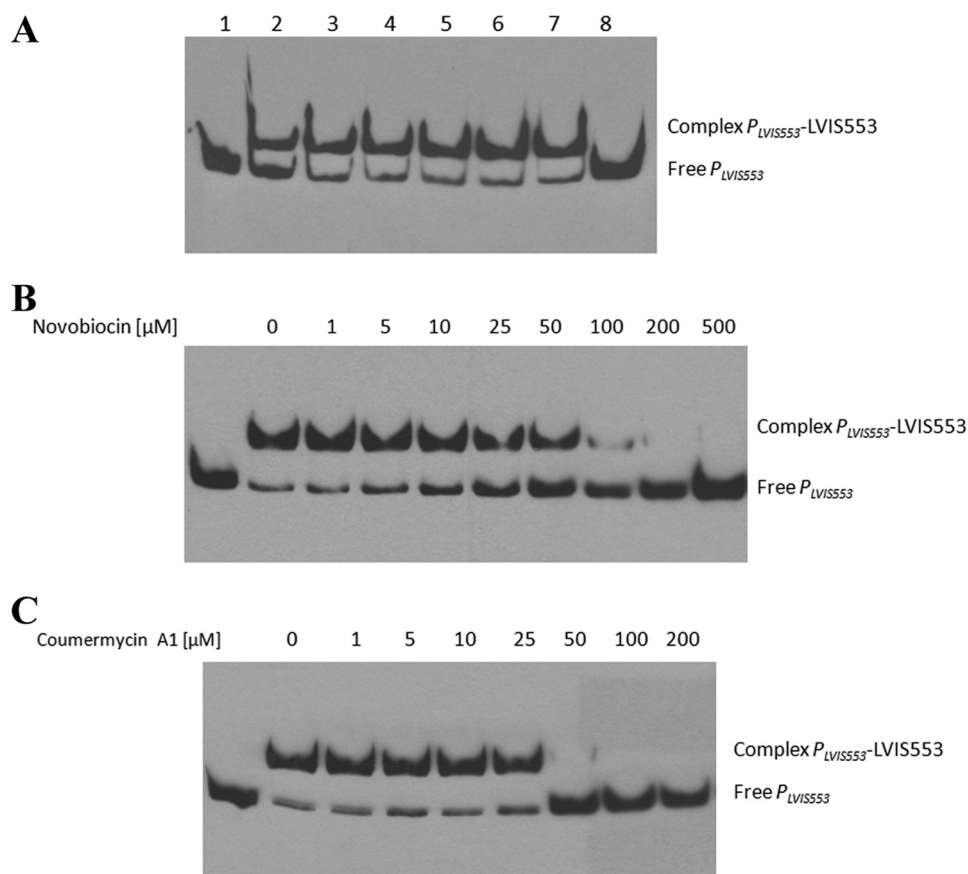
A

B

C

FIGURE 3. **Effect of different small molecules on LVIS553 binding to $P_{LVIS553}$.** EMSA results using 2.5 nM biotin-labeled $P_{LVIS553}$ and 10 nM LVIS553 with different inducer molecules (*A*) or with increasing concentrations of novobiocin (*B*) or coumermycin A1 (*C*). No protein was added to the first lane. The full binding conditions are described under "Experimental Procedures." In *A*, *lane 1* shows the migration of the target DNA fragment; *lanes 2–7*, LVIS553 at 10 nM. Carbamezepine (*lane 3*), canrenoic acid (*lane 4*), diazoxide (*lane 5*), pindolol (*lane 6*), zomepirac (*lane 7*), and novobiocin (*lane 8*) were added at a concentration of 100 μM.

a drastic shift in the amino acid charge, LVIS553 K9D, also resulted in decreased affinity for DNA (Fig. 7*A*) and no effect of novobiocin was observed (data not shown).

LVIS553 K9D showed binding of $P_{LVIS553}$ to the DNA fragment at 10 nM (as the wild type). Concentrations of novobiocin up to 1 mM had a very slight effect on the LVIS553 K9D·$P_{LVIS553}$ complex (Fig. 7*B*), suggesting that Lys[9] is the residue involved in binding to novobiocin. The residual ligand binding activity observed might be mediated by weak interactions with other residues in the binding cavity.

The effect of the LVIS553 K9D mutant was tested *in vivo* using *B. subtilis* as a surrogate, due to technical difficulties associated with the genetic manipulation of *L. brevis* ATCC367. The genes *LVIS552-LVIS553* (or its mutant variant K9D) were cloned in pSac-Kan and integrated in the *sacA* gene of *B. subtilis* M168. The tolerance to novobiocin was increased by 10-fold in *B. subtilis LVIS552-LVIS553* when compared with *B. subtilis sacA*::Kan[r] (empty vector integrated at the *sacA* locus as control), with a minimal inhibitory concentration of 5 and 0.5 μM, respectively. The high tolerance to novobiocin conferred by LVIS552 was reverted when LVIS553 was mutated in Lys[9] (Fig. 4*B*). These results confirmed the role of Lys[9] as the amino acid involved in the specific binding of novobiocin.

DISCUSSION

In this report we took an unbiased approach, using high throughput screening of small molecules library, to identify novobiocin as the specific effector molecule for LVIS553. *In silico* modeling of LVIS553 identified MTH313 (PDB code 3BPX) (2) as the closest structural homolog. MTH313 is one of the few available structures with its ligand as salicylate, which shed light into the mechanism of interaction of the small molecule/protein. Interestingly, the physiologically relevant SAL1 is found in the interface of the dimerization domain and DNA binding domain, making it difficult to discriminate residues involved in DNA binding, ligand binding, or both. A detailed analysis performed in SlyA identified several amino acids within the winged-helix region, as well as two hydrophobic residues (Leu[12] and Leu[126]) within α1 and α6 that are required for DNA binding (4). Using structure-guided mutagenesis, we aimed to identify residues involved in ligand binding within the SAL1 cavity. Arg[16] is highly conserved among different MarR members. We found that an alanine substitution (LVIS553 R16A) resulted in impaired DNA binding, suggesting a role in sequence recognition.

On the contrary, Lys[9] is only conserved in homologs close to LVIS553, indicating that Lys[9] may be the regulatory residue involved in the specific binding of novobiocin. LVIS553 K9A showed similar affinity for DNA as the wild type strain, whereas no further response to novobiocin was detected. Although it is speculated that the SAL1 cavity has the potential to bind a wide variety of small molecules, LVIS553 only bound novobiocin or the closely related molecule coumermycin A1. The determined affinity constants for novobiocin were in the low micromolar range, consistent with a molecule having physiological relevance. These *in vitro* results were correlated with the *in vivo* induction in gene expression of *LVIS553* and its downstream gene *LVIS552*, a putative membrane protein.

The antibacterial property of novobiocin is well established in the literature. It targets the DNA gyrase activity that translates into pleiotropic effects on the cell, affecting DNA replication, DNA repair, recombination, and ultimately cell growth (37). The novobiocin biosynthetic cluster of *Streptomyces caeruleus* is positively regulated by NovG and NovE (38). NovG is an unusual transcription factor with a predicted central helix-
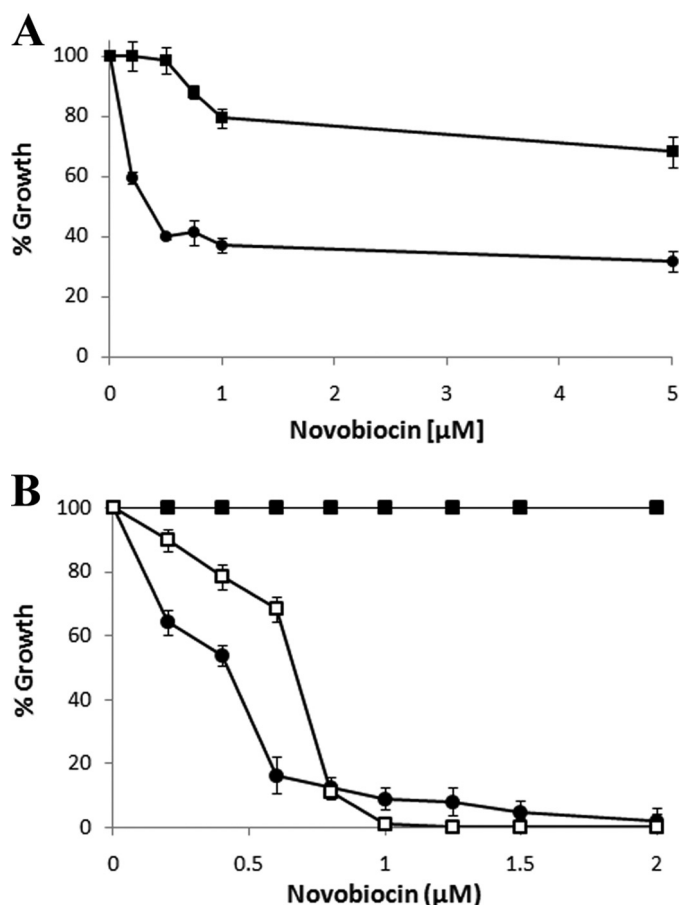
A

B

FIGURE 4. **Heterologous expression of *LVIS552* and *LVIS553* in *L. brevis* and *B. subtilis*.** *A*, *L. brevis* cells were grown with increasing concentrations of novobiocin in the presence (*closed squares*) or absence (*closed circles*) of *LVIS552-LVIS553* cloned in pRV610. *B*, growth of *B. subtilis* with a chromosomal insertion of *LVIS552-LVIS553* in the *sacA* locus (*closed squares*), empty controls (kanamycin cassette in the *sacA* locus, *closed circles*), and *LVIS552-LVIS553* (K9A) mutant (*open squares*). Growth was expressed as a percentage of the OD of cells grown without novobiocin.

FIGURE 5. **Isothermal titration calorimetric data for the binding of novobiocin to LVIS553.** Heat changes (*upper panel*) and integrated peak areas (*lower panel*) for the injection of a series of 4-μl aliquots of 1 mM ligand in a solution of 40 μM protein. Protein solutions at 40 μM in 10 mM HEPES, pH 7.5, and 500 mM NaCl were titrated with 1 mM solution of effector. Experiments were carried out at 30 °C.

turn-helix DNA binding domain that specifically recognizes the sequence GTTCRACTG(N)$_{11}$CRGTYGAAC (39). The effect of novobiocin on NovG binding properties, if any, has not yet been reported.

We identified the DNA binding sequence for LVIS553 using footprinting assay. The protected region is 30 nucleotides long and located on the minus strand, upstream of *LVIS553,* overlapping the predicted -10 region of the *LVIS553* promoter. It includes a 7-bp imperfect palindrome (5′-TAaTGGActtaTC-CAcTA-3′) flanked on both sides by AT-rich sequences. A competitive EMSA with the 30-nucleotide fragment confirmed the specificity of this region. A similar arrangement of the binding sequence has been described for two other MarR members, MepR (40) and OhrR (41).

The identification of new mechanisms of tolerance to antibiotics is very relevant. Novobiocin in particular, has been suggested as a treatment for Gram-positive infections in penicillin-resistant strains (42). Different mechanisms of tolerance to novobiocin have been described including mutations on the DNA gyrase (33) and the activation of multidrug efflux pumps (5). In *L. brevis,* the expression in *trans* of *LVIS552-LVIS553* results in an increased tolerance to
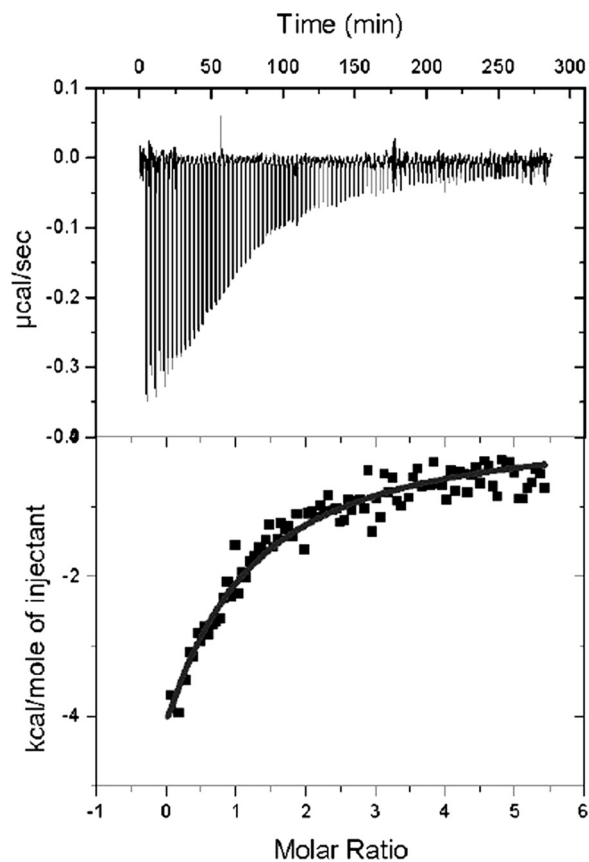
novobiocin, indicating that the putative membrane protein LVIS552 is involved in detoxification of novobiocin. These results were confirmed using *B. subtilis* as a surrogate strain. We revealed that the heterologous expression of *LVIS552* increased the tolerance to novobiocin 4-fold. In *B. subtilis,* the multidrug efflux transporter MdtP (YusP) was associated with increased tolerance to several antibiotics, including fusidic acid, novobiocin, streptomycin, and actinomycin D (5). Similarly to LVIS552, the expression of MdtP is regulated by MdtR (YusO), a MarR member encoded upstream of the multidrug efflux transporter (YusP). Kim *et al.* (5) reported that mutations in the regulatory protein MdtR (R83K or A67T) impaired DNA binding and resulted in a 2-fold increase in tolerance to streptomycin, actinomycin D, and novobiocin, as well as a 5-fold increase in tolerance to fusidic acid. Interestingly, EMSA experiments with MdtR revealed binding affinities in the millimolar range for novobiocin and fusidic acid, questioning their biological significance.

In conclusion, we provide evidence that LVIS553 is involved in the specific regulation of a new mechanism of tolerance to novobiocin. In contrast to the other MarR members that respond to "preconceived" ligands (*i.e.* salycilate) that have been studied, we provide *in vitro* data that correlates with *in vivo* responses. The identification of key resi-
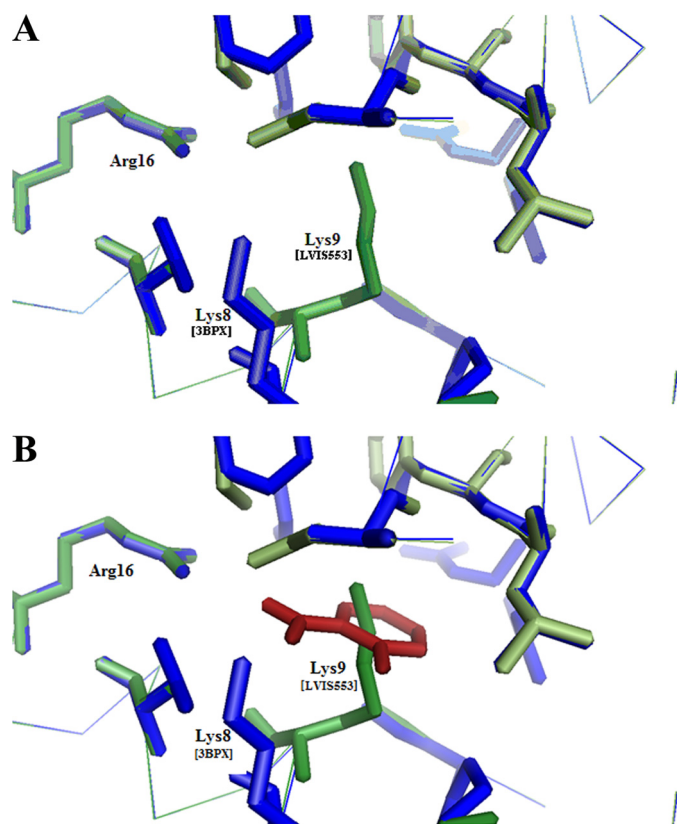
FIGURE 6. **Close view (6-Å radius) of the SAL1 binding site of MTH313 (PDB code 3BPX) (2) aligned with the predicted model for LVIS553.** *A*, model of the LVIS553 structure (in *green*) constructed using MTH313 (in *blue*) as a template. *B*, salicylate from MTH313 (in *red*) is displayed.
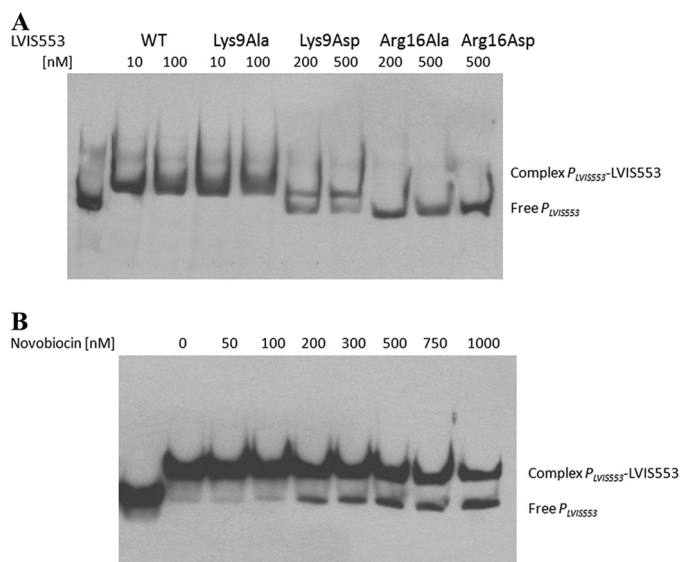

FIGURE 7. **Distinctive functions of Lys⁹ and Arg¹⁶ residues identified by EMSA.** *A*, DNA binding properties of LVIS553 substitution mutants. *WT*, wild type protein. *B*, effect of novobiocin on the stability of LVIS553-K9A·$P_{LVIS553}$ complex.

dues involved in specific binding of small molecules, contributes not only to the growing body of knowledge currently needed to decipher the intricate mechanism of interactions between the signal molecules and MarR, but may also serve as a starting point for the design of innovative therapeutics in the near future.

REFERENCES

1. Alekshun, M. N., Levy, S. B., Mealy, T. R., Seaton, B. A., and Head, J. F. (2001) *Nat. Struct. Biol.* **8,** 710–714
2. Saridakis, V., Shahinas, D., Xu, X., and Christendat, D. (2008) *J. Mol. Biol.* **377,** 655–667
3. Alekshun, M. N., Kim, Y. S., and Levy, S. B. (2000) *Mol. Microbiol.* **35,** 1394–1404
4. Okada, N., Oi, Y., Takeda-Shitaka, M., Kanou, K., Umeyama, H., Haneda, T., Miki, T., Hosoya, S., and Danbara, H. (2007) *Microbiology* **153,** 548–560
5. Kim, J. Y., Inaoka, T., Hirooka, K., Matsuoka, H., Murata, M., Ohki, R., Adachi, Y., Fujita, Y., and Ochi, K. (2009) *J. Bacteriol.* **191,** 3273–3281
6. Seoane, A. S., and Levy, S. B. (1995) *J. Bacteriol.* **177,** 3414–3419
7. Martin, R. G., and Rosner, J. L. (1995) *Proc. Natl. Acad. Sci. U.S.A.* **92,** 5456–5460
8. Alekshun, M. N., and Levy, S. B. (1999) *J. Bacteriol.* **181,** 4669–4672
9. Yu, L., Fang, J., and Wei, Y. (2009) *Biochemistry* **48,** 2099–2108
10. Wilkinson, S. P., and Grove, A. (2006) *Curr. Issues Mol. Biol.* **8,** 51–62
11. Brooun, A., Tomashek, J. J., and Lewis, K. (1999) *J. Bacteriol.* **181,** 5131–5133
12. Wilkinson, S. P., and Grove, A. (2004) *J. Biol. Chem.* **279,** 51442–51450
13. Wilkinson, S. P., and Grove, A. (2005) *J. Mol. Biol.* **350,** 617–630
14. Pérez-Rueda, E., Collado-Vides, J., and Segovia, L. (2004) *Comput. Biol. Chem.* **28,** 341–350
15. Lorca, G. L., and Font de Valdez, G. (2009) in *Lactobacillus Molecular Biology: From Genomics to Probiotics* (Ljungh, A., and Wadström, T., eds) pp. 115–137, Caister Academic Press, Norfolk, UK
16. Simpson, W. J., and Fernandez, J. L. (1992) *Lett. Appl. Microbiol.* **14,** 13–16
17. Sakamoto, K., Margolles, A., van Veen, H. W., and Konings, W. N. (2001) *J. Bacteriol.* **183,** 5371–5375
18. Suzuki, K., Iijima, K., Ozaki, K., and Yamashita, H. (2005) *Appl. Environ. Microbiol.* **71,** 5089–5097
19. Makarova, K., Slesarev, A., Wolf, Y., Sorokin, A., Mirkin, B., Koonin, E., Pavlov, A., Pavlova, N., Karamychev, V., Polouchine, N., Shakhova, V., Grigoriev, I., Lou, Y., Rohksar, D., Lucas, S., Huang, K., Goodstein, D. M., Hawkins, T., Plengvidhya, V., Welker, D., Hughes, J., Goh, Y., Benson, A., Baldwin, K., Lee, J. H., Díaz-Muñiz, I., Dosti, B., Smeianov, V., Wechter, W., Barabote, R., Lorca, G., Altermann, E., Barrangou, R., Ganesan, B., Xie, Y., Rawsthorne, H., Tamir, D., Parker, C., Breidt, F., Broadbent, J., Hutkins, R., O'Sullivan, D., Steele, J., Unlu, G., Saier, M., Klaenhammer, T., Richardson, P., Kozyavkin, S., Weimer, B., and Mills, D. (2006) *Proc. Natl. Acad. Sci. U.S.A.* **103,** 15611–15616
20. Lorca, G. L., Barabote, R. D., Zlotopolski, V., Tran, C., Winnen, B., Hvorup, R. N., Stonestrom, A. J., Nguyen, E., Huang, L. W., Kim, D. S., and Saier, M. H., Jr. (2007) *Biochim. Biophys. Acta* **1768,** 1342–1366
21. Sambrook, J., Fritsch, E. F., and Maniatis, T. (1989) *Molecular Cloning: A Laboratory Manual*, 2nd Ed., Cold Spring Harbor Laboratory, Cold Spring Harbor, NY
22. Crutz-Le Coq, A. M., and Zagorec, M. (2008) *Plasmid* **60,** 212–220
23. Middleton, R., and Hofmeister, A. (2004) *Plasmid* **51,** 238–245
24. Petit-Glatron, M. F., and Chambert, R. (1992) *J. Gen. Microbiol.* **138,** 1089–1095
25. Lorca, G. L., Ezersky, A., Lunin, V. V., Walker, J. R., Altamentova, S., Evdokimova, E., Vedadi, M., Bochkarev, A., and Savchenko, A. (2007) *J. Biol. Chem.* **282,** 16476–16491
26. Zianni, M., Tessanne, K., Merighi, M., Laguna, R., and Tabita, F. R. (2006) *J. Biomol. Tech.* **17,** 103–113
27. Vedadi, M., Niesen, F. H., Allali-Hassani, A., Fedorov, O. Y., Finerty, P. J., Jr., Wasney, G. A., Yeung, R., Arrowsmith, C., Ball, L. J., Berglund, H., Hui, R., Marsden, B. D., Nordlund, P., Sundstrom, M., Weigelt, J., and Edwards,

A. M. (2006) *Proc. Natl. Acad. Sci. U.S.A.* **103,** 15835–15840

28. Niesen, F. H., Berglund, H., and Vedadi, M. (2007) *Nat. Protoc.* **2,** 2212–2221

29. Wiseman, T., Williston, S., Brandts, J. F., and Lin, L. N. (1989) *Anal. Biochem.* **179,** 131–137

30. Saier, M. H., Jr., Yen, M. R., Noto, K., Tamang, D. G., and Elkan, C. (2008) *Nucleic Acids Res.* **37,** 274–278

31. Nobeli, I., and Thornton, J. M. (2006) *BioEssays* **28,** 534–545

32. Senisterra, G. A., Markin, E., Yamazaki, K., Hui, R., Vedadi, M., and Awrey, D. E. (2006) *J. Biomol. Screen* **11,** 940–948

33. Hooper, D. C., Wolfson, J. S., McHugh, G. L., Winters, M. B., and Swartz, M. N. (1982) *Antimicrob. Agents Chemother.* **22,** 662–671

34. Schwede, T., Kopp, J., Guex, N., and Peitsch, M. C. (2003) *Nucleic Acids Res.* **31,** 3381–3385

35. Arnold, K., Bordoli, L., Kopp, J., and Schwede, T. (2006) *Bioinformatics* **22,** 195–201

36. Altschul, S. F., Madden, T. L., Schäffer, A. A., Zhang, J., Zhang, Z., Miller, W., and Lipman, D. J. (1997) *Nucleic Acids Res.* **25,** 3389–3402

37. Jackson, A. P., and Maxwell, A. (1993) *Proc. Natl. Acad. Sci. U.S.A.* **90,** 11232–11236

38. Dangel, V., Eustáquio, A. S., Gust, B., and Heide, L. (2008) *Arch. Microbiol.* **190,** 509–519

39. Eustáquio, A. S., Li, S. M., and Heide, L. (2005) *Microbiology* **151,** 1949–1961

40. Kumaraswami, M., Schuman, J. T., Seo, S. M., Kaatz, G. W., and Brennan, R. G. (2009) *Nucleic Acids Res.* **37,** 1211–1224

41. Hong, M., Fuangthong, M., Helmann, J. D., and Brennan, R. G. (2005) *Mol. Cell.* **20,** 131–141

42. Gombert, M. E., and Aulicino, T. M. (1984) *Antimicrob. Agents Chemother.* **26,** 933–934

43. Thompson, J. D., Higgins, D. G., and Gibson, T. J. (1994) *Nucleic Acids Res.* **22,** 4673–4680